Effect of Chiral Cavities Associated with Molecularly Imprinted Platinum Centers on the Selectivity of Ligand-Exchange Reactions at Platinum

Nicole M. Brunkan and Michel R. Gagné*

Contribution from the Department of Chemistry, CB #3290, University of North Carolina, Chapel Hill, North Carolina 27599-3290

Received February 7, 2000

Abstract: The metallomonomer (vinyl dppe)Pt[(*R*)-Bu_2BINOL] (**1**) was copolymerized with ethylene glycol dimethacrylate to produce the molecularly imprinted polymer (MIP) **P1**. The chiral imprinting ligand (*R*)-Bu_2BINOL was removed from **P1** by treatment with HCl or an excess of α,α,α-trifluoro-*m*-cresol, BINOL, or Br_2BINOL, giving polymers **P2**−**P5**. The amount of imprinting ligand released from **P1** varied inversely with the steric bulk of the cleaving agent, indicating that a distribution of Pt sites with different accessibilities exists in the MIP. Exposure of **P3** (containing $Pt(OAr)_2$ centers surrounded by (*R*)-Bu_2BINOL-shaped cavities) to *rac*-BINOL, an imprinting ligand analogue, led to preferential rebinding of the imprinted enantiomer via ligand exchange. Both aggregate selectivity and extent of reaction (percent of the total Pt sites in the MIP that participated in rebinding) increased with rebinding time and with temperature, up to 69% ee and 58% Pt sites rebound, respectively. A positive linear correlation between selectivity and reactivity was observed. Open, easily accessible Pt sites were proposed to be less selective than unreactive sites because their associated chiral cavities are less well-defined and therefore less capable of shape-based enantiodiscrimination. The kinetic selectivity of the *least reactive* sites in **P3** was assessed by sequential rebinding of *rac*-BINOL and then *rac*-Br_2BINOL. Rebound BINOL was recovered from 8 to 20% of the least reactive Pt sites accessible in the MIP in 89−94% ee. All data indicate that chiral cavities (outer sphere) associated with the reactive Pt centers in these MIPs are responsible for the selectivities observed for stoichiometric ligand-exchange reactions at the metal center.

Introduction

The enantioselectivity of many asymmetric catalytic reactions stems from the catalyst's ability to control the orientation with which a substrate binds to the active center. In synthetic catalysts, bulky chiral ligands coordinated to the metal center (*inner sphere*) influence binding and subsequent reactivity by blocking specific regions of space around the catalyst. Metalloenzymes, on the other hand, utilize the *outer sphere* (residues that surround but are not coordinated to the active metal) as well as the inner sphere to control binding events. This suggests that a synthetic catalyst's selectivity could be improved by better defining its outer sphere.

In conventional homogeneous catalysis, the outer sphere consists of the dynamic, ill-defined solvent shell, making outer-sphere stereocontrol impractical. However, several chiral transition metal ligands have been developed that utilize pseudo-outer-sphere functionalities, projected into space around the region of substrate binding to the metal center, to enhance the selectivity of reactions occurring at the metal.[1] These ligands are thought to be highly selective because the functionalized arms either interact with and guide incoming nucleophiles or they influence the orientation of a bound substrate through ion pairing effects. The success of these ligands in asymmetric catalysis suggests that outer-sphere interactions can significantly contribute to the stereochemical outcome of transition metal-catalyzed reactions.

A biomimetic approach to controlling the outer sphere of a transition metal catalyst is to encase the catalyst in an organic or inorganic matrix, which provides an outer sphere for the metal center in the same way that a protein forms the outer sphere of an enzyme active site.[2] The methodology best suited for creation of such a catalyst is *molecular imprinting*, which involves incorporation of a template into a highly cross-linked, yet porous organic polymer. First reported by Wulff in the early 1970s, the molecular imprinting technique has been extensively developed and reviewed.[3] Molecularly imprinted polymers (MIPs) that incorporate chiral organic templates have received the most attention due to their application as chiral chromatographic

(1) Selected examples: (a) Hayashi, T. In *Catalytic Asymmetric Synthesis*; Ojima, I., Ed.; VCH Publishers: New York, 1993; pp 325−365. (b) Sawamura, M.; Ito, Y. In *Catalytic Asymmetric Synthesis*; Ojima, I., Ed.; VCH Publishers: New York, 1993; pp 367−388. (c) Sawamura, M.; Nagata, H.; Sakamoto, H.; Ito, Y. *J. Am. Chem. Soc.* **1992**, *114*, 2586−2592. (d) Armspach, D.; Matt, D. *Chem. Commun.* **1999**, 1073−1074. (e) Collman, J. P.; Zhang, X.; Lee, V. J.; Uffelman, E. S.; Brauman, J. I. *Science* **1993**, *261*, 1404−1411. (f) Sanders, J. K. M. *Chem. Eur. J.* **1998**, *4*, 1378−1383.

(2) Davis, M. E.; Katz, A.; Ahmad, W. R. *Chem. Mater.* **1996**, *8*, 1820−1839.

(3) (a) Ramström, O.; Ansell, R. J. *Chirality* **1998**, *10*, 195−209. (b) Brady, P. A.; Sanders, J. K. M. *Chem. Soc. Rev.* **1997**, *26*, 327−336. (c) Wulff, G. *Angew. Chem., Int. Ed. Engl.* **1995**, *34*, 1812−1832. (d) Shea, K. J. *Trends Polym. Sci.* **1994**, *2*, 166−173. (e) Mosbach, K. *Trends Biochem. Sci.* **1994**, 9−14. (f) Wulff, G. In *Polymeric Reagents and Catalysis*; Ford, W. T., Ed.; American Chemical Society: Washington, DC, 1986; pp 186−230. (g) Sherrington, D. C. *Chem. Commun.* **1998**, 2275−2286.

10.1021/ja000462c CCC: $19.00
Published on Web 06/02/2000

Scheme 1

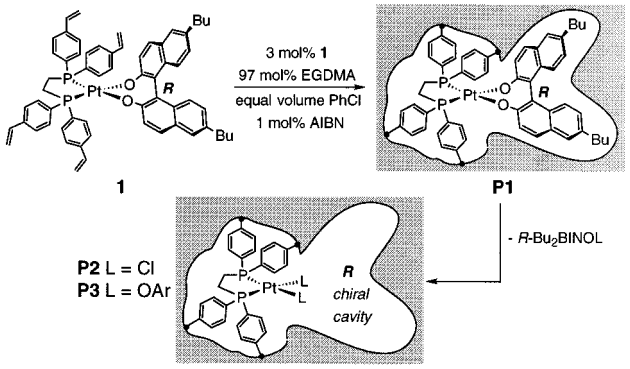

stationary phases, but catalytically active organic MIPs have also been produced by Shea,[4] Wulff,[5] and Mosbach.[6] These MIP catalysts consist of general acids and bases precisely positioned within cavities imprinted by a transition-state analogue (TSA) to catalyze a target organic transformation.

Metal-containing MIPs have also been developed and used for catalysis,[2,7] molecular recognition,[7d,8] and reactive complex isolation.[9] In the area of catalysis, Mosbach has demonstrated that Co-containing polymers imprinted with the shape of an aldolate TSA catalyze the aldol condensation,[7a] while Severin has utilized polymers imprinted with an organometallic TSA Ru complex to catalyze the transfer hydrogenation of aromatic ketones.[7c] With respect to molecular recognition, Fujii has shown that imprinted chiral cavities associated with polymer-bound chiral metal complexes contribute up to 3 kcal mol^{-1} toward recognition of the imprinted enantiomer during rebinding reactions.[7d] This last example suggests that suitable combinations of chiral catalyst (inner sphere) and chiral cavity (outer sphere) working in tandem in a MIP could provide extremely high enantioselectivities in asymmetric catalysis.

Herein we describe use of the molecular imprinting methodology to create imprinted chiral cavities associated with achiral, polymer-bound transition metal complexes, and we demonstrate that these associated cavities can impart high selectivity to reactions that occur at the metal center. Scheme 1 illustrates how the imprinting strategy can be utilized to generate a transition metal complex with an experimentally definable outer sphere. Imprinting template **1** consists of a polymerizable *linking ligand*, 1,2-bis(di-4-styrylphosphino)ethane (vinyl dppe), and a nonpolymerizable *imprinting ligand*, (*R*)-6,6′-dibutyl-1,1′-bi-2-naphthol [(*R*)-Bu_2BINOL], coordinated to a square planar Pt(II) center. Copolymerization of metallomonomer **1** with an organic cross-linking agent leads to covalent incorporation (through the vinyl groups on the linking ligand) of **1** into a highly cross-linked polymer. Chemical removal of the chiral imprinting ligand then reveals chiral cavities in the polymer, each associated with a platinum center in a spatially precise manner. The effect of these associated chiral cavities (outer sphere) on the stereoselectivity of stoichiometric ligand-exchange reactions that occur at the Pt centers can then be investigated. This research constitutes a first step toward creation of a fundamentally new type of immobilized transition metal catalyst whose outer sphere controls its selectivity.

Results and Discussion

(1) Template and Polymer Synthesis. The linking ligand (vinyl dppe) was prepared in 72% yield by addition of the Grignard reagent 4-styrylmagnesium chloride[10] to 1,2-bis-(dichlorophosphino)ethane. The bulky, axially chiral (*R*)-1,1′-bi-2-naphthol [(*R*)-BINOL] was initially chosen as imprinting ligand because its chirality is manifested in a sterically obvious manner (*R* and *S* enantiomers have very different shapes). However, the complex (vinyl dppe)Pt[(*R*)-BINOL] (analogous to **1**) proved insoluble in most common organic solvents, so *n*-butyl groups were added to the BINOL ligand to enhance the template's solubility. Nickel-catalyzed Grignard coupling of *n*-butylmagnesium bromide with methoxy-protected (*R*)-6,6′-dibromo-1,1′-bi-2-naphthol [(*R*)-Br_2BINOL] afforded the more soluble imprinting ligand in 75% overall yield.[11] Yellow metallomonomer **1** was prepared from (vinyl dppe)$PtCO_3$ and (*R*)-Bu_2BINOL in 92% yield by a procedure analogous to that published for non-vinyl analogues.[12]

Free-radical polymerization of **1** with the cross-linker ethylene glycol dimethacrylate (EGDMA) in the presence of an equal volume of porogen (chlorobenzene = PhCl) yielded a transparent, orange-yellow polymer monolith **P1** (Scheme 1). The polymerization was thermally initiated by AIBN under a nitrogen atmosphere and allowed to proceed for 48 h at 60 °C. The product polymer, which was stable toward air and water, was manually broken into small pieces with a spatula[13] and dried in vacuo for 12 h, giving opaque **P1** containing 130 μmol of Pt/g of polymer. The extremely high degree of cross-linking makes **P1** rigid, hard, and insoluble in everything, including aqua regia. However, the polymer also possesses a permanent pore structure, as indicated by its extremely high surface area (427 $m^2\ g^{-1}$),[14] which allows rapid diffusion of substrates within the polymer matrix.

Attempted characterization of the solid **P1** by $^{31}P\{^1H\}$ CP/MAS-HP NMR yielded a spectrum with a single, extremely broad (3200-Hz line width at half-height) resonance centered at the same chemical shift as that of **1** in CH_2Cl_2 solution.[15] However, the width of the peak precluded differentiation of Pt satellites from the main resonance. This led us to suspect that any small impurities present within ±30 ppm of the main resonance would also be undetectable, as they would lie under the "umbrella" of the broad main peak. Indeed, $^{31}P\{^1H\}$ CP/MAS-HP spectra of MIPs **P2** and **P3**, which are each composed of a mixture of two polymer-bound Pt species (vide infra),

(4) Beach, J. V.; Shea, K. J. *J. Am. Chem. Soc.* **1994**, *116*, 379−380.
(5) Wulff, G.; Gross, T.; Schönfeld, R. *Angew. Chem., Int. Ed. Engl.* **1997**, *36*, 1962−1964.
(6) (a) Liu, X.-C.; Mosbach, K. *Macromol. Rapid Commun.* **1997**, *18*, 609−615. (b) Robinson, D. K.; Mosbach, K. *J. Chem. Soc., Chem. Commun.* **1989**, 969−970.
(7) (a) Matsui, J.; Nichols, I. A.; Karube, I.; Mosbach, K. *J. Org. Chem.* **1996**, *61*, 5414−5417. (b) Locatelli, F.; Gamez, P.; Lemaire, M. *J. Mol. Catal. A: Chem.* **1998**, *135*, 89−98. (c) Polborn, K.; Severin, K. *Chem. Commun.* **1999**, 2481−2482. (d) Fujii, Y.; Matsutani, K.; Kikuchi, K. *Chem. Commun.* **1985**, 415−417.
(8) (a) Matsui, J.; Tachibana, Y.; Takeuchi, T. *Anal. Commun.* **1998**, *35*, 225−227. (b) Dahl, P. K.; Arnold, F. H. *J. Am. Chem. Soc.* **1991**, *113*, 7417−7418. (c) Suh, J.; Cho, Y.; Lee, K. J. *J. Am. Chem. Soc.* **1991**, *113*, 4198−4202.
(9) (a) Krebs, J. F.; Borovik, A. S. *Chem. Commun.* **1998**, 553−554. (b) Krebs, J. F.; Borovik, A. S. *J. Am. Chem. Soc.* **1995**, *117*, 10593−10594.
(10) Rabinovich, R.; Marcus, R. *J. Org. Chem.* **1961**, *26*, 4157−4158.
(11) Supporting Information from: Sasai, H.; Tokunaga, T.; Watanabe, S.; Suzuki, T.; Itoh, N.; Shibasaki, M. *J. Org. Chem.* **1995**, *60*, 7388−7389.
(12) Full details of syntheses of **1** and precursors are given in the Supporting Information.
(13) The MIP particles used in experiments were ≤2 mm/edge but were not of uniform size. To minimize loss of material, sieving was not performed.
(14) Determined for a typical **P1** sample from N_2 adsorption isotherms by application of the BET theory (see Experimental Section). Average pore diameter was 45 Å; pore volume distribution measurements showed that the majority of pores have diameters less than 100 Å and can thus be classified as micro- (<20 Å diameter) or mesopores (20−500 Å diameter).

Scheme 2

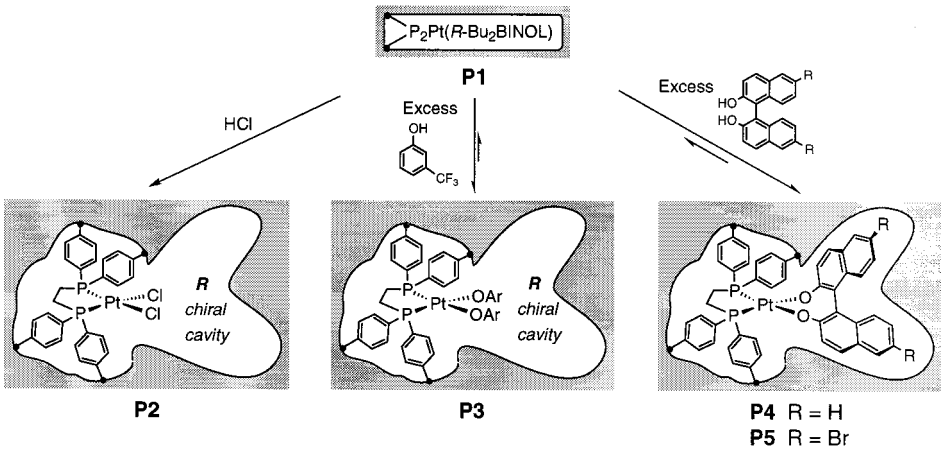

showed only one broad resonance each, centered at the chemical shift of the major species. To date, $^{31}P\{^{1}H\}$ CP/MAS-HP NMR has not proven useful as a characterization tool for polymers with the high cross-link densities necessary for molecular imprinting.[16]

Because direct characterization of **P1** by NMR proved impractical, the integrity of Pt complex **1** after polymerization was demonstrated by synthesizing a non-vinyl analogue of **1** and subjecting it to the free-radical polymerization conditions. The non-vinyl analogue was not cross-linked into the polymer and could be recovered unharmed following the experiment.

(2) Removal of the Imprinting Ligand (*R*)-Bu$_2$BINOL. Several ways to remove the imprinting ligand from **P1** (and thereby reveal the chiral cavities associated with imprinted Pt centers) were investigated (Scheme 2). In a typical experiment, insoluble **P1** was treated with a solution of the active reagent in CH_2Cl_2 or PhCl. The reagent solution was then filtered from the polymer and used for the Soxhlet extraction of cleaved (*R*)-Bu$_2$BINOL from the treated polymer. The amount of (*R*)-Bu$_2$BINOL in the solution recovered from the Soxhlet apparatus was determined by quantitative HPLC analysis. At least three different batches of **P1** were subjected to each treatment in order to establish the reproducibility of the experimental method and evaluate batch-to-batch variability in the MIPs.

The first (*R*)-Bu$_2$BINOL removal method explored involved cleaving the ligand from Pt with HCl. Immersion of yellow **P1** in a dilute solution of aqueous HCl in CH_2Cl_2 for 6 h caused the polymer to gradually turn white, the color of the solution analogue (vinyl dppe)$PtCl_2$, indicating formation of **P2**. Generally 83 ± 1% of the theoretical amount of imprinting ligand in **P1** was released upon treatment with HCl. A second general way to remove (*R*)-Bu$_2$BINOL from **P1** was suggested by the observation that non-vinyl analogues of **1** undergo ligand-exchange reactions in solution; (*R*)-Bu$_2$BINOL is displaced from Pt by acidic phenols or BINOL analogues. It was anticipated that a large excess of phenol or BINOL could be used to drive the exchange equilibrium toward new $Pt(OAr)_2$ or Pt(BINOL) species, thus releasing (*R*)-Bu$_2$BINOL from the polymer. Indeed, immersion of **P1** in neat α,α,α-trifluoro-*m*-cresol (HOAr) at 100 °C for 10−24 h generated the polymer **P3** and liberated 67 ± 2% of the (*R*)-Bu$_2$BINOL contained in the starting material. Similarly, exposure of **P1** to a 0.1 M solution of BINOL or Br$_2$BINOL (8 equiv with respect to the theoretical number of Pt sites in the polymer) in PhCl for 4 h at 60 °C displaced 27 ± 1 and 31 ± 1%, respectively, of the imprinting ligand in **P1** and generated the polymers **P4** and **P5**.

These experiments indicate that the amount of (*R*)-Bu$_2$BINOL displaced from **P1** *decreases* as the steric bulk of the ligand displacing it *increases*.[17] Assuming that the ligand-exchange reactions proceed by proton transfer from the outgoing to the incoming ligand (both ligands must simultaneously be in close proximity to the platinum center),[18] this trend implies that a *distribution* of platinum sites with different accessibilities to bulky reagents exists in the MIP. Only 30% of the Pt sites (the most reactive) are open enough to permit the approach of BINOL or Br$_2$BINOL to a Pt center with (*R*)-Bu$_2$BINOL already coordinated to it. On the other hand, 67% of the sites can accommodate both (*R*)-Bu$_2$BINOL and HOAr near the Pt center, and 83% permit the approach of the smaller, more acidic HCl molecule to the Pt[(*R*)-Bu$_2$BINOL] site. The imprinting ligand stays trapped in the remaining (least reactive) 17% of imprinted Pt sites upon treatment with all reagents. However, the fact that HCl-treated **P1** completely loses its yellow color suggests that (*R*)-Bu$_2$BINOL can be cleaved from all Pt sites in the MIP but that the bulky ligand cannot escape from the least accessible sites due to diffusional restrictions.

(15) $^{31}P\{^{1}H\}$ CP/MAS-HP NMR was performed on a Bruker DMX 360-MHz instrument with spinning rate 9−10 kHz, 2-dB ^{1}H decoupling power, 1400−2400 scans/spectrum. The excessive peak broadening probably occurs because these MIPs are so highly cross-linked and rigid that even MAS cannot sufficiently homogenize the phosphorus nuclei in different polymer environments. By contrast, P_2PtX_2 complexes immobilized in polymers with cross-link densities of ≤50% give resonances with narrow (100 Hz) line widths. See: (a) Fyfe, C. A.; Clark, H. C.; Davies, J. A.; Hayes, P. J.; Wasylishen, R. E. *J. Am. Chem. Soc.* **1983**, *105*, 6577−6584. (b) Bemi, L.; Clark, H. C.; Fyfe, C. A.; Wasylishen, R. E. *J. Am. Chem. Soc.* **1982**, *104*, 438−445.

(16) Valuable ^{13}C CP/MAS data for MIPs has, however, been obtained by Shea. See: Shea, K. J.; Sasaki, D. Y. *J. Am. Chem. Soc.* **1991**, *113*, 4109−4120.

(17) Reagent steric bulk is not the sole factor that determines the extent of ligand exchange in the polymer; reagent acidity also plays an important role. Solution ligand-exchange experiments performed with non-vinyl analogues of **1** showed that the position of the exchange equilibrium (K_{eq}) depends largely on the relative acidities of the ligands involved: coordination of strongly acidic ligands to Pt is favored over coordination of less acidic ones (manuscript in progress). For a careful analysis of the kinetics of this phenomenon see: Simpson, R. D.; Bergman, R. G. *Organometallics* **1993**, *12*, 781−796.

(18) The ligand-exchange mechanism probably involves preequilibrium hydrogen bonding of the incoming phenol or diol to the Pt aryloxide oxygen. ^{31}P NMR spectra of (dppe)Pt[(*R*)-BINOL] show that the complex's chemical shift depends on the amount of free BINOL present in solution, suggesting that H-bonding is occurring. See: (a) Andrews, M. A.; Cook, G. K.; Shriver, Z. H. *Inorg. Chem.* **1997**, *36*, 5832−5844. (b) Kim, Y.-J.; Osakada, K.; Takenaka, A.; Yamamoto, A. *J. Am. Chem. Soc.* **1990**, *112*, 1096−1104. (c) Kegley, S. E.; Schaverien, C. J.; Freudenberger, J. H.; Bergman, R. G.; Nolan, S. P.; Hoff, C. D. *J. Am. Chem. Soc.* **1987**, *109*, 6563−6565. (d) Bugno, C. D.; Pasquali, M.; Leoni, P.; Sabatino, P.; Braga, D. *Inorg. Chem.* **1989**, *28*, 1390−1394. (e) See ref 17.

Scheme 3

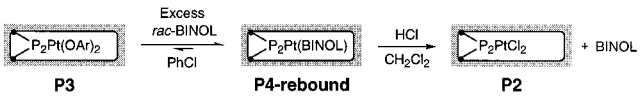

The heterogeneity of imprinted sites in molecularly imprinted polymers has previously been discussed and is often compared to the distribution of active site structures in polyclonal antibodies.[2,3] Because the EGDMA building blocks used to define the template's imprint in the polymer are of the same order of magnitude in size as the template itself, positioning of the cross-linked polymer chains around the template is necessarily imprecise, and imprints with varying degrees of fidelity are produced.[3c]

(3) Rebinding of *rac*-BINOL to P3. To assess the effect of imprinted chiral cavities on the selectivity of ligand-exchange reactions at the associated Pt centers, the (*R*)-Bu_2BINOL-imprinted polymer **P3** was exposed to *racemic* BINOL, an imprinting ligand analogue (Scheme 3). **P3** is ideal for rebinding studies because the Pt-coordinated aryl oxide ligands in the imprinted sites can easily be displaced by the chelating imprinting ligand (or structural analogue) using the same exchange reaction employed to remove (*R*)-Bu_2BINOL (Scheme 2). Addition of excess rebinding ligand drives the exchange equilibrium toward the desired rebound Pt species. *rac*-BINOL was used for rebinding instead of *rac*-Bu_2BINOL because not *all* the original imprinting ligand could be removed from the polymer during preparation of **P3**; thus rebound BINOL could be analyzed separately from (*R*)-Bu_2BINOL left in the polymer during the template removal step (vide infra).

In each rebinding experiment, immersion of **P3** in a PhCl solution containing excess (13 equiv with respect to $Pt(OAr)_2$ sites) *rac*-BINOL (0.1 M) led to BINOL displacement of some of the coordinated aryl oxide. After excess unbound BINOL was washed from **P4**-rebound by Soxhlet extraction, the polymer was treated with HCl to release the rebound BINOL and give **P2**. During this step, (*R*)-Bu_2BINOL from sites that are inaccessible to HOAr but accessible to HCl was also liberated from the polymer, but it was easily separated from rebound BINOL during HPLC analysis of the mixture of cleaved ligands.[19] The solution obtained from Soxhlet extraction of **P2** was analyzed quantitatively by chiral stationary phase HPLC, giving the amount and percent ee of rebound BINOL. The percentage (*n*) of the total Pt sites in the polymer that were rebound by BINOL was calculated from the former. The percent ee represents the *average selectivity* of the *most reactive n*% of the total Pt sites in the polymer. To establish the consistency of the analysis methods, the amount of (*R*)-Bu_2BINOL liberated from the rebound polymer was determined and added to the amount of (*R*)-Bu_2BINOL released during preparation of **P3** from **P1**, giving the total amount of (*R*)-Bu_2BINOL recovered from the original **P1**. A total of 84 ± 2% of the imprinting ligand could usually be accounted for, in good agreement with the 83% released by direct cleavage of **P1** with HCl.

(4) Effect of Rebinding Time on the Reactivity and Selectivity of Rebinding Reactions. As anticipated, (*R*)-Bu_2BINOL-imprinted polymers exposed to *rac*-BINOL preferentially rebound the imprinted *R* enantiomer.[20] Both the reactivity(percent of total Pt sites rebound) and the selectivity of the MIPs depended on the conditions under which the rebinding reaction (Scheme 3) was carried out.[21] The effect of rebinding time on reactions performed at 40 °C is shown in Figure 1. Although the rebinding reaction is heterogeneous, it proceeded surprisingly quickly; the maximum number of Pt sites rebound (45%) was reached in ~2 h. Selectivity for the imprinted *R* enantiomer increased with time (to a maximum of 61% ee) and with percent Pt sites rebound.

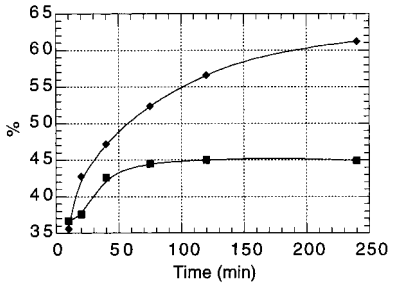

Figure 1. Percent of total Pt sites in **P3** rebound by *rac*-BINOL (■) and percent ee of rebound BINOL (◆) as a function of rebinding time for rebinding reactions (Scheme 3) performed at 40 °C.

The observation that reaction selectivity increases as more Pt sites in the MIP become involved in the rebinding reaction strongly suggests that the ability of an imprinted chiral cavity to distinguish between enantiomers of the imprinted ligand is linked to its accessibility. We hypothesized that *the accessibility of a given Pt site depends on the level of outer-sphere definition of its associated chiral cavity*, such that Pt centers associated with loosely defined, open cavities are easily accessible to incoming reagents, whereas Pt centers with extremely well-defined cavities are so tightly bounded by polymer as to be completely unreactive. Furthermore, sites with well-defined chiral cavities (good memory of the imprinting ligand) were expected to exhibit greater recognition of the imprinted enantiomer than sites with poorly defined cavities. It follows that easily accessible, highly reactive Pt sites in the MIP should exhibit poor selectivity for the imprinted enantiomer during a rebinding reaction, while less accessible, less reactive Pt sites should be capable of much greater selectivity. The MIP behavior described by Figure 1 (Pt sites that react most quickly are least selective, whereas sites that react increasingly slowly are increasingly more selective) is consistent with this hypothesis. Note that this behavior is opposite to that of other MIPs reported in the literature (discussion in section 8).[22]

Interestingly, the selectivity of the rebinding reaction continued to increase at reaction times longer than 2 h, although no net additional BINOL was incorporated into the polymer.[23] This trend indicates that the polymer's thermodynamic selectivity exceeds its kinetic selectivity and suggests that two reactions are occurring simultaneously within the polymer (Scheme 4).

(19) No racemization of the (*R*)-Bu_2BINOL was observed under these reaction conditions. Similarly, the enantiomeric purity of (*R*)-BINOL was unaffected by vigorous refluxing in a dilute solution of aqueous HCl in CH_2Cl_2 for 24 h.

(20) Similar experiments with (*S*)-Bu_2BINOL-imprinted polymers result in preferential rebinding of (*S*)-BINOL. (*S*)-Bu_2BINOL MIPs behave identically to (*R*)-Bu_2BINOL MIPs except for opposite percent ee.

(21) These reaction conditions include rebinding time (section 4), rebinding temperature (section 5), and rebinding solvent [not addressed here because preliminary experiments indicate that solvent effects on the rebinding reaction (Scheme 3) are small]. Note, however, that MIPs used as chromatographic stationary phases often exhibit decreased selectivity when solvents other than the porogen used to prepare the MIP are employed as the mobile phase: (a) Spivak, D.; Gilmore, M. A.; Shea, K. J. *J. Am. Chem. Soc.* **1997**, *119*, 4388−4393. (b) Allender, C. J.; Heard, C. M.; Brain, K. R. *Chirality* **1997**, *9*, 238−242. Also, when rebinding occurs via hydrogen bonding of the template to the MIP, solvent polarity greatly affects rebinding selectivity. See refs 2 and 3.

(22) (a) Wulff, G.; Grobe-Einsler, R.; Vesper, W.; Sarhan, A. *Makromol. Chem.* **1977**, *178*, 2817−2825. (b) Sarhan, A. *Makromol. Chem.* **1989**, *190*, 2031−2039. (c) Shea, K. J.; Sasaki, D. Y. *J. Am. Chem. Soc.* **1991**, *113*, 4109−4120.

(23) A similar situation was observed in ref 22b.

Scheme 4

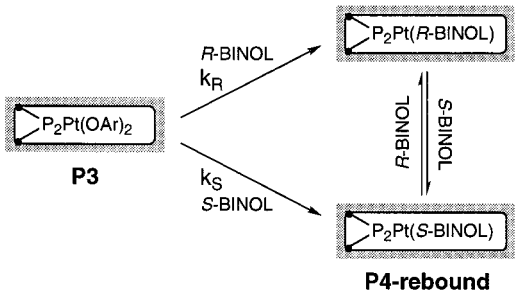

The first reaction comprises initial displacement of coordinated aryloxide by (*R*)- or (*S*)-BINOL (left half of Scheme 4). Under the conditions employed for rebinding (excess BINOL), this reaction is rapid and effectively irreversible[24] and occurs with a *kinetic* selectivity that reflects the rate difference k_R/k_S. Once (*R*)- or (*S*)-BINOL has been bound to a Pt center within a chiral cavity, exchange of free (*R*)-BINOL with coordinated (*S*)-BINOL (and vice versa) also occurs in the more accessible sites. The free energy for this exchange reaction is zero in solution, but nonzero in the MIP environment, due to the different stabilities of Pt[(*R*)-BINOL] within an *R* chiral cavity (favorable matched case) and Pt[(*S*)-BINOL] in an *R* chiral cavity (less favorable mismatched case). Thus, *thermodynamic* selectivity is also possible in the MIP. BINOL−BINOL exchange is proposed to account for the increase in selectivity observed at longer reaction times, as (*R*)-BINOL slowly displaces Pt-coordinated (*S*)-BINOL in the polymer.

BINOL−BINOL exchange during the rebinding reaction is postulated to occur analogously to BINOL and Br_2BINOL exchange with the (*R*)-Bu_2BINOL in **P1** (Scheme 2, section 2).[25] Since these reagents displace (*R*)-Bu_2BINOL from only 30% of the Pt sites in **P1**, it is unlikely that all of the 45% of Pt sites occupied by BINOL in **P4**-rebound are able to undergo BINOL−BINOL exchange. Only Pt sites with open, accessible chiral cavities are expected to be under thermodynamic control; sites associated with more well-defined and selective cavities remain under kinetic control. Thus, the overall selectivity (% ee) of the rebinding reaction is an aggregate that represents not only a range of selectivities for sites with different discriminatory abilities but also a mixture of kinetic selectivity for some sites and thermodynamic selectivity for others.

Additional experiments to establish the reproducibility of Figure 1 showed similar data trends, although some batch-to-batch variability in MIP performance was observed. In some experiments, the percent of Pt sites rebound after 2 h increased slowly over time (up to 8 h). After 8 h, selectivity stabilized at 65−70% ee.

(5) Effect of Rebinding Temperature on the Reactivity and Selectivity of Rebinding Reactions. Figure 2 shows the effect of temperature on the extent of reaction and aggregate selectivity for rebinding reactions in which **P3** was subjected to *rac*-BINOL (Scheme 3) for 4 h at a series of temperatures

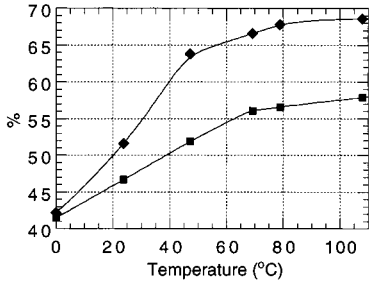

Figure 2. Percent of total Pt sites in **P3** rebound by *rac*-BINOL (■) and percent ee of rebound BINOL (◆) as a function of temperature for rebinding reactions (Scheme 3) carried out for 4 h.

ranging from 0 to 110 °C. Contrary to the norm for conventional reactions carried out in solution, selectivity of the rebinding reaction *increased* with increasing temperature, and with percent Pt sites rebound.[26] This trend demonstrates that increasingly less reactive but more selective Pt sites become available to BINOL at higher temperatures. Note that, at temperatures below 40 °C, BINOL−aryl oxide (OAr) exchange reactions are not expected to be complete under the chosen experimental conditions after only 4 h reaction time. Thus, the percent Pt sites rebound does not represent the total number of sites accessible at that temperature, but only the number of sites accessible *in 4 h reaction time*. Likewise, equilibrium between polymer-bound Pt[(*R*)-BINOL] and Pt[(*S*)-BINOL] complexes is achieved in 4 h at temperatures above 40 °C, but not at lower temperatures. Thus, the different selectivities observed for reactions conducted between 50 and 110 °C reflect the establishment of different equilibria involving different numbers of Pt sites; the different selectivities observed for reactions carried out between 0 and 40 °C occur because BINOL−OAr and BINOL−BINOL exchange reactions are more or less complete. In both cases, the net effect is that accessing a greater number of Pt sites in the MIP enhances reaction selectivity.

(6) Reactivity/Selectivity Correlation. Taken together, all the data obtained from rebinding experiments (Scheme 3) in which *rac*-BINOL was allowed to react with **P3** at various temperatures, for various lengths of time, clearly illustrate that aggregate MIP selectivity depends primarily on extent of reaction (Figure 3). In fact, the relationship between selectivity (expressed as aggregate enantiomeric ratio, *R*/*S*) and reactivity (percent Pt sites rebound) is roughly linear when 35−60% of the total Pt sites have been rebound. It should be emphasized that kinetic and thermodynamic data obtained at multiple temperatures have been combined in Figure 3. Although we see no a priori reason why kinetic selectivity should depend on reactivity in exactly the same way that thermodynamic selectivity does, it appears that both correlate with percent Pt sites rebound in the same manner (all data points lie on the same line).

The relatively steep slope of the line suggests that each newly accessed imprinted site is significantly more selective than the one reacting immediately before it. Because the measured selectivity of the rebinding reaction (enantiomeric ratio) at a given conversion (percent Pt sites rebound) is an *aggregate selectivity*, or average over all Pt sites in the polymer that have reacted at that conversion, it is surprising that it increases substantially with small increases in conversion. This means

(24) Although BINOL is less acidic than 3-CF_3PhOH (2-naphthol pK_a = 17.14, while 3-CF_3PhOH pK_a = 15.6; see Bordwell, F. G.; Cheng, J.-P. *J. Am. Chem. Soc.* **1991**, *113*, 1736−1743), the solution equilibrium (dppe)Pt(3-CF_3PhO)$_2$ + BINOL ↔ (dppe)Pt(BINOL) + 2 3-CF_3PhOH lies far to the right due to the chelate effect. K_{eq} = 720 for the solution exchange reaction (manuscript in progress).

(25) The selectivities associated with these exchange reactions, carried out at 60 °C, were measured by cleavage of the BINOL or Br_2BINOL ligands from **P4** and **P5** with HCl. Quantitative chiral HPLC analysis of the recovered ligands revealed that BINOL binds on average to 27% of the total Pt sites in **P4** with 46 ± 1% ee, while Br_2BINOL generally occupies 31% of the total Pt sites in **P5** with 36 ± 1% ee.

(26) The selectivity of other MIPs has been observed to increase with temperature in both batch rebinding and chromatographic experiments, see for example: (a) Wulff, G.; Vietmeier, J.; Poll, H.-G. *Makromol. Chem.* **1987**, *188*, 731−740. (b) Wulff, G.; Schauhoff, S. *J. Org. Chem.* **1991**, *56*, 395−400. (c) Wulff, G.; Poll, H.-G.; Minárik, M. *J. Liq. Chromatogr.* **1986**, *9*, 385−405. (d) Sellergren, B. *Makromol. Chem.* **1989**, *190*, 2703−2711.

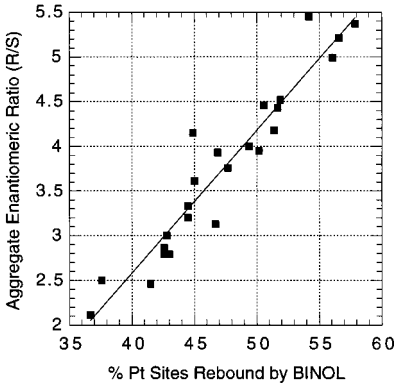

Figure 3. Selectivity (aggregate enantiomeric ratio, *R/S*) as a function of reactivity (percent Pt sites rebound by BINOL) for the rebinding of *rac*-BINOL to **P3**. Individual data points were generated by carrying out the rebinding reaction shown in Scheme 3 under different conditions (rebinding time and temperature); reaction temperatures varied from 0 to 110 °C, and rebinding times varied from 5 min to 8 h. The best-fit line is drawn as an aid to the eye and is not intended to imply a mathematical model.

that the *additional* Pt sites accessed at high conversion (a relatively small number compared to the number of sites accessed at low conversion) are so much more selective than the initially reacting sites that they compensate for the poor selectivity of the latter and raise the overall average selectivity significantly. This rough interpretation of Figure 3 proved useful in the design of subsequent rebinding experiments; however, development of a physically relevant mathematical model to describe the reactivity/selectivity relationship was not practical because of the complexity of the data set (combination of kinetics, thermodynamics, and averages over a continuous distribution of sites).

(7) Kinetic Selectivity of the *Least Reactive* Imprinted Sites. The kinetic selectivity of the subset of rebound Pt sites in **P4**-rebound that are *amenable to BINOL−aryl oxide but not BINOL−BINOL exchange* was evaluated experimentally as shown in Scheme 5. After washing away excess BINOL left from the standard *rac*-BINOL rebinding reaction (60 °C for 4 h) by Soxhlet extraction, **P4**-rebound was allowed to react with *rac*-Br_2BINOL (a second imprinting ligand analogue) under the same conditions, except that the second rebinding temperature was varied from 60 to 100 °C. Br_2BINOL thus displaced BINOL from sites able to accommodate such exchange, but left behind BINOL in less accessible, presumably more selective sites. After excess unbound ligand was removed from **P4/5**-rebound by Soxhlet extraction, all ligands were cleaved from the polymer with HCl. The ligands in a solution recovered from Soxhlet extraction of the cleaved polymer were quantitatively analyzed by chiral HPLC to determine the percent Pt sites rebound by BINOL and Br_2BINOL (*m* and *n*%, respectively) and the percent ee of each rebound ligand.[27] The Br_2BINOL percent ee represents the average *thermodynamic* selectivity of the *n*% *most reactive* Pt sites in the polymer, while the BINOL percent ee reflects the average *kinetic* selectivity of the *m*% *least reactive* sites accessible in the polymer.

The disparity between the BINOL and Br_2BINOL percent ee's listed in Table 1 clearly demonstrates that less reactive Pt sites are far more selective than easily accessible sites. For example, thermodynamic selectivity of the Pt sites amenable to Br_2BINOL exchange at 60 °C was 46% ee, while kinetic selectivity of nonexchangeable sites was 89% ee. Increasing Br_2BINOL rebinding temperature increased the number of Pt sites able to accommodate BINOL−Br_2BINOL exchange, so less BINOL was left behind in **P4/5**-rebound. Br_2BINOL percent ee increased in the usual manner as more Pt sites reacted with Br_2BINOL at higher rebinding temperatures. BINOL percent ee was also expected to increase with Br_2BINOL rebinding temperature as fewer, increasingly well-defined Pt sites in **P4/5**-rebound were left occupied by BINOL. A substantial increase in percent ee was observed on comparison of the selectivity of the 13% least reactive Pt sites with that of the 20% least reactive sites. However, the least reactive 8% of Pt sites accessible to BINOL were not significantly more selective than the least reactive 13%. This may indicate that the selectivity limit of the imprinted polymer lies around 94% ee. In this case, the most selective chiral cavities accessible in the MIP could contribute ~2.5 kcal mol^{-1} kinetic selectivity ($\Delta\Delta G^{\ddagger}$) toward enantiodiscrimination of a (pro)chiral substrate during a catalytic asymmetric reaction at their associated transition metal sites.

(8) Contrast of Observed Reactivity/Selectivity Correlation with Previously Described MIP Reactivity/Selectivity Relationships. The data from sections 4−7 indicate that the most reactive sites in the Pt MIPs investigated are also the least selective. Although this correlation makes logical sense for the reaction of a well-shaped ligand with a single metal buried in a cavity, the opposite behavior is normally observed[22] (or assumed) for other MIPs. For example, the most reactive sites in MIPs generated from diketal templates (**A**) are also those

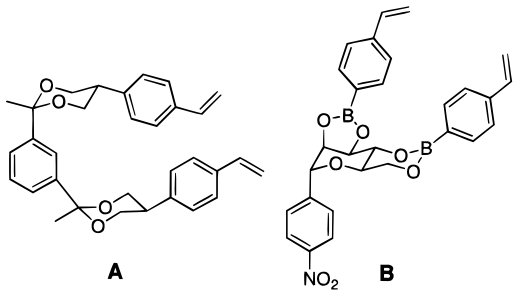

most likely to reketalize diketones in a two-point fashion.[22c] Similarly, the most reactive imprinted sites generated by homochiral sugar diboronate ester templates (**B**) are those most capable of discriminating between the sugar enantiomers in batch rebinding and in chromatography.[22a] These observations point to a situation in which mutual enhancements in reactivity and selectivity are caused by preequilibrium noncovalent binding interactions between difunctional substrates and complementarily difunctionalized MIP sites.[28] Though this recognition/activation process is not well understood, it is apparently most important in reactions involving rapid preequilibration prior to an irreversible stereodefining event. Since the cavities of the Pt MIPs described herein are not multifunctional, this preequilibrium scenario does not apply. Instead, the more readily rationalized idea that cavity *shape* is responsible for the inverse relationship between reactivity and selectivity has been proposed. Note, however, that Pt MIPs containing a second functional group in the chiral cavity might be expected to show the more commonly observed direct correlation between reactivity and selectivity.

(27) (*R*)-Bu_2BINOL, (*R*)- and (*S*)-BINOL, and (*R*)- and (*S*)-Br_2BINOL could all be separated on a Daicel OD-H chiral column with 5%EtOH/hexanes mobile phase. See Supporting Information for a typical chromatogram.

(28) For an exception in which an MIP containing one functional group per cavity gave rise to a similar trend (selectivity increases with reactivity), see ref 22b.

Scheme 5

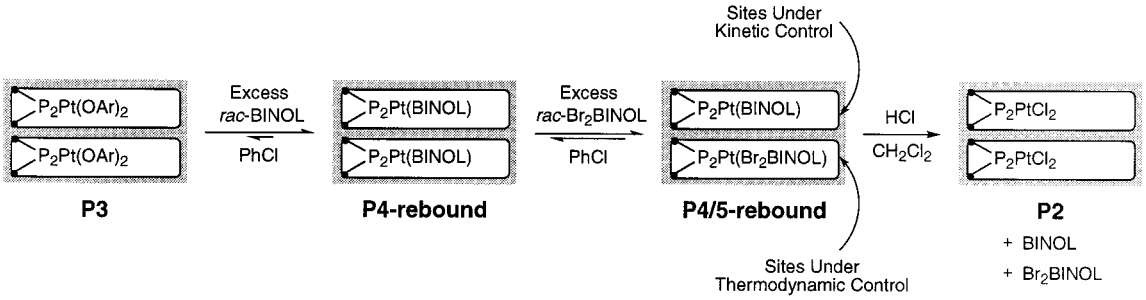

Table 1. Data for the Sequential Rebinding of *rac*-BINOL and Then *rac*-Br_2BINOL to **P3** (Scheme 5)

Br_2BINOL rebinding temp (°C)	% Pt sites bound by Br_2BINOL	Br_2BINOL % ee	% Pt sites bound by BINOL	BINOL % ee	% Pt sites rebound (total)
60	41	46	20	89	61
80	46	58	13	94	59
100	50	61	8	94	58

(9) Associated Chiral Cavities versus Induced Chiral Conformation in the Diphosphine Linking Ligand. Previously published studies showed that interaction of (*R*)-BINOL with 1,2-bis(diphenylphosphino)ethane (dppe) across the Pt square plane in (dppe)Pt[(*R*)-BINOL] tends to induce the λ skew conformation in the achiral diphosphine in the solid state.[29] It is thus possible that the phosphine might be "locked" into this conformation upon incorporation of a vinyl analogue into a highly cross-linked polymer (Scheme 6). If the rigid polymer surrounding the ligand sufficiently impairs its movement, the phosphine could retain a chiral conformation after the imprinting ligand (*R*)-Bu_2BINOL is removed, effectively transforming the achiral ligand into a chiral one. A proviso to this argument is that freezing of the λ/δ interconversion in dppe derivatives is rare and has only been observed on the NMR time scale at low temperatures.[30] Nevertheless, solution ligand-exchange experiments using Pt complexes of the dppe analogue (*S*,*S*)-chiraphos were undertaken to evaluate the effect of a chiral diphosphine on the selectivity of the exchange reaction (Scheme 7).[31] At the polymerization temperature (60 °C), the chiral diphosphine contributes only 0.4 kcal mol^{-1} toward thermodynamic selectivity for the matched BINOL enantiomer over the mismatched. This contribution can account for at most 28% ee, generally lower than the selectivities demonstrated by the MIPs described here. Dependence of selectivity on reactivity is also inconsistent with an inner-sphere mechanism of stereoselectivity. Thus, the data indicate that the selectivity observed for BINOL rebinding to Pt in these MIPs can be primarily attributed to the outer-sphere effects of the chiral cavities associated with reactive Pt centers rather than to the inner-sphere effects of a potentially chiral diphosphine linking ligand.

Conclusions

Platinum template complexes containing an achiral linking ligand and a chiral imprinting ligand can be incorporated into highly cross-linked organic polymers, and the imprinting ligand can be removed by cleavage with HCl or exchange with acidic phenols or BINOL analogues. The amount of imprinting ligand released by treatment of a MIP with a given reagent is inversely related to the steric bulk of that reagent, implying that a distribution of Pt sites with varying accessibilities exists within the polymer. Removal of the imprinting ligand reveals chiral cavities in the MIP, each associated with a reactive Pt center, which range from poorly to highly enantioselective for the recognition of imprinting ligand analogues during stoichiometric ligand-exchange reactions at the Pt centers.

Aggregate MIP selectivity increases as more imprinted Pt sites participate in a rebinding reaction, indicating that less accessible Pt sites are more selective than sites that react quickly. This behavior implies that the accessibility of a Pt site depends on the degree of outer-sphere definition of the chiral cavity associated with it: Pt sites surrounded by spacious, vaguely defined cavities afford little selectivity because their outer spheres are imprecisely shaped, whereas sites bounded by well-defined cavities show excellent recognition of the imprinted enantiomer. Measurement of the kinetic selectivity of the *least reactive* Pt sites in the MIP reveals that selectivities up to 94% ee can be realized through predominantly *outer-sphere* effects. However, the aggregate selectivity of the MIP decreases considerably to ~65% ee when the effects of all sites, both reactive and unreactive, are taken into account.

These conclusions have dramatic consequences for our goal of utilizing imprinted metal complexes for asymmetric catalysis: the least selective sites will be the most reactive and will

Scheme 6

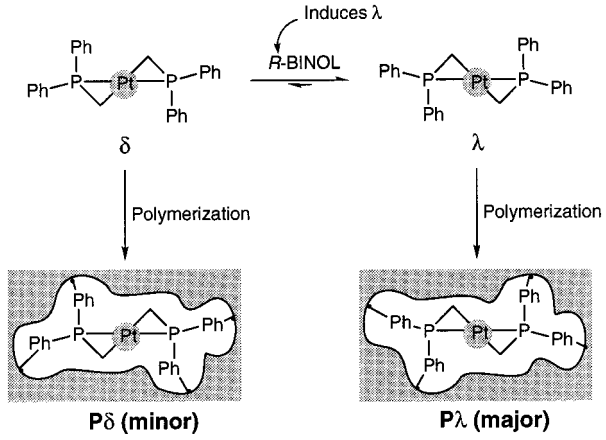

Scheme 7

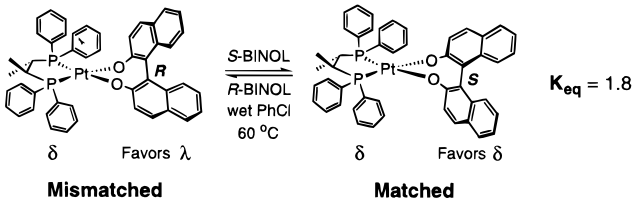

(29) Brunkan, N. M.; White, P. S.; Gagné, M. R. *Angew. Chem., Int. Ed.* **1998**, *37*, 1579−1582.

(30) Ohkita, K.; Kurosawa, H.; Hirao, T.; Ikeda, I. *J. Organomet. Chem* **1994**, *470*, 179−182.

(31) For the reaction in Scheme 7, $K_{eq} = 3.6$ in dry CH_2Cl_2 at room temperature. See ref 29.

therefore dominate the imprinted catalyst's product output! To rectify this undesirable situation, we envision selective poisoning of the most accessible, least selective sites (conceptually similar to the way Br_2BINOL was used in the present work to separate imprinted Pt sites into subsets exhibiting high and low selectivity; section 7). Addition of a substoichiometric amount (with respect to the number of metal sites in the MIP) of a large, strongly binding diphosphine or other ligand to a transition metal catalyst-imprinted polymer will irreversibly deactivate the open, ill-defined sites and direct reactivity to the remaining sites with well-shaped outer spheres. The notion of poisoning hyperreactive sites to reveal the more selective ones has previously been employed to enhance the selectivity of steroidal MIP HPLC supports.[32]

Experimental Section

General Methods. Typical polymer syntheses and rebinding experiments are described here; for syntheses of **1** and precursors see Supporting Information. All chemicals were purchased from Aldrich. Chlorobenzene (PhCl) was distilled from P_2O_5 and freeze−pump−thaw degassed before use as a porogen, but was used as received in rebinding experiments. 2,2′-Azobis(isobutyro)nitrile (AIBN) was recrystallized from MeOH, dried in vacuo, and stored under N_2 at −35 °C. EGDMA was washed twice with aqueous 1 M NaOH and once with brine to remove inhibitor, dried over $MgSO_4$, filtered, distilled (105 °C/1 mmHg), freeze−pump−thaw degassed, and stored under N_2 at −35 °C.[21a] α,α,α-Trifluoro-*m*-cresol was distilled (30 °C/0.03 mmHg) and stored under Ar, but still contained ≤5% impurity (probably a positional isomer) by HPLC. Polymerizations were performed in an MBraun LabMaster 100 glovebox. Reactions done under N_2 or Ar were carried out using standard Schlenk techniques. HPLC was performed on a Hewlett-Packard Series 1100 instrument, using Daicel Chiralcel OJ or OD-H columns (Chiral Technologies) for chiral work and a LiChrospher 100 CN column (Hewlett-Packard) for achiral work. Polymer analyses were performed by Robertson Microlit Laboratories, Madison, NJ (Pt quantitation by ICP).

Polymer surface area and pore volume distribution analysis was carried out at Dupont CR&D, Wilmington, DE. Dinitrogen adsorption/desorption measurements were performed at 77.3 K on Micrometrics ASAP model 2400/2405 porosimeters. A typical sample of **P1** (1.2 g, broken into pieces ≤2 mm/edge) was degassed at 150 °C under vacuum for 16 h prior to data collection. A five-point adsorption isotherm collected over 0.05−0.20 p/p_0 was analyzed via the BET method[33] to give surface area data; a 27-point desorption isotherm analyzed via the BJH method[34] was used to determine pore volume distribution.

During polymer experiments, all Soxhlet extractions were performed for at least 6 h. All polymer intermediates in a reaction sequence were dried in vacuo for at least 2 h before use in subsequent reaction steps. Quantitation of ligands present in a solution obtained from Soxhlet extraction of a polymer was accomplished using the following procedure: Solvent was removed in vacuo. The residue was quantitatively transferred to a volumetric flask and diluted with a known volume of ^{i}PrOH. HPLC chromatograms of the sample were recorded at wavelengths 289, 278, 254, and 333 nm and compared to calibration curves to determine analyte concentration.

P1. Metallomonomer **1** (170.8 mg, 156.1 μmol), AIBN (8.5 mg, 51.8 μmol), EGDMA (1.007 g, 5080 μmol), and PhCl (1.0540 g) were combined in a 20-mL scintillation vial under N_2 and sealed with a Teflon-lined cap. The vial was heated to 60 °C for 48 h, yielding a hard, transparent, yellow-orange polymer. After drying in vacuo at 50 °C for 17 h, 1.22 g of polymer (including 31 mg of PhCl not removed by drying; 128.4 μmol of Pt/g of polymer) was obtained. Anal. Calcd for **P1**: Pt, 2.47. Found: Pt, 2.36.

P2. Eight drops of concentrated HCl(aq) were added to a suspension of yellow **P1** (0.19 g, 24.5 μmol of Pt) in CH_2Cl_2 (15 mL). The polymer gradually turned white while being stirred at room temperature. After 6 h, the polymer was filtered from solution and transferred to a glass Soxhlet thimble; the filtrate was transferred to a round-bottom flask and used for Soxhlet extraction (15 h) of the polymer. Quantitative HPLC analysis (CN column; 5% ^{i}PrOH/hexanes) of the extract showed that 20.1 μmol of (*R*)-Bu_2BINOL was recovered from the polymer (83.2% of the total Pt sites in **P1**). After drying in vacuo at 150 °C for 36 h, 0.17 g of white **P2** was obtained. Anal. Calcd for **P2**: Pt, 2.55; Cl, 0.78. Found: Pt, 2.52; Cl, 1.06.

P3. α,α,α-Trifluoro-*m*-cresol (2 mL) was added to a flask equipped with a reflux condenser, charged with **P1** (0.20 g, 26.2 μmol of Pt) under vacuum, and allowed to degas. Water (0.5 mL)[35] was added under Ar, and the reaction mixture was stirred for 17 h at 100 °C. The polymer was then filtered from hot solution, rinsed with CH_2Cl_2, transferred to a glass Soxhlet thimble, and extracted for 6 h using the filtrate (with additional CH_2Cl_2) as extraction solution. Following removal of excess α,α,α-trifluoro-*m*-cresol from the extract by distillation in vacuo, quantitative HPLC analysis (CN column; 5% ^{i}PrOH/hexanes) of the residue showed that 17.0 μmol of (*R*)-Bu_2BINOL was recovered from the polymer (64.8% of the total Pt sites in **P1**). After drying for 36 h in vacuo at 150 °C,[36] 0.20 g of pale yellow **P3** was obtained. Anal. Calcd for **P3**: Pt, 2.53; F, 0.96. Found: Pt, 2.38; F, 0.53.

P4. PhCl (2 mL) and water (0.5 mL) were added to a flask equipped with a reflux condenser and charged with **P1** (0.20 g, 25.9 μmol of Pt) and *rac*-BINOL (62.4 mg, 218 μmol). The reaction mixture was stirred for 4 h at 60 °C under Ar. The polymer was then filtered from hot solution, transferred to a glass Soxhlet thimble, and extracted for 18 h using the filtrate as extraction solution. Quantitative HPLC analysis (CN column; 5% ^{i}PrOH/hexanes) of the extract showed that 6.25 μmol of (*R*)-Bu_2BINOL was recovered from the polymer (24.1% of the total Pt sites in **P1**). The yellow polymer was dried in vacuo for 9 h, giving 0.19 g of **P4**, which was then cleaved with HCl to give **P2** using the same procedure as for synthesis of **P2** from **P1**. Quantitative chiral HPLC analysis (OJ column, 20% ^{i}PrOH/hexanes) of the final Soxhlet extract showed that 6.82 μmol of BINOL (27.2% of the total Pt sites in **P4**; 45.6% ee) and an additional 15.6 μmol of (*R*)-Bu_2BINOL [62.2% of the total Pt sites in **P4**; total, (*R*)-Bu_2BINOL was removed from 86.3% of the Pt sites of the original **P1**] were recovered from the polymer.

P5. This was prepared in the same way as **P4** from 0.21 g of **P1** (27.7 μmol of Pt) and 106 mg of *rac*-Br_2BINOL (238 μmol). Quantitative HPLC analysis (CN column; 5% ^{i}PrOH/hexanes) of the first Soxhlet extract showed that 8.04 μmol of (*R*)-Bu_2BINOL was recovered from the polymer (29.0% of the total Pt sites in **P1**). The yellow polymer was dried in vacuo for 8 h, giving 0.21 g of **P5**, which was cleaved with HCl to give **P2**. Quantitative chiral HPLC analysis (OD-H column, 12% ^{i}PrOH/hexanes) of the final Soxhlet extract showed that 8.10 μmol of Br_2BINOL (30.5% of the total Pt sites in **P5**; 37.0% ee) and an additional 15.5 μmol of (*R*)-Bu_2BINOL [58.4% of the total Pt sites in **P5**; total, (*R*)-Bu_2BINOL was removed from 87.4% of the Pt sites of the original **P1**] were recovered from the polymer.

Typical *rac*-BINOL Rebinding Experiment. PhCl (2 mL) and water (0.5 mL) were added to a flask equipped with a reflux condenser and charged with **P3** [0.19 g, 24.0 μmol of total Pt, 16.6 μmol of $Pt(OAr)_2$] and *rac*-BINOL (61.8 mg, 216 μmol). The reaction mixture was stirred for 4 h at 69 °C under Ar. The polymer was then filtered from hot solution, transferred to a glass Soxhlet thimble, and extracted with CH_2Cl_2 for 18 h. After drying in vacuo for 4 h, 0.18 g of yellow **P4**-rebound was obtained. This polymer was cleaved with HCl to give **P2**. Quantitative chiral HPLC analysis (OJ column, 20% ^{i}PrOH/

(32) McNiven, S.; Yokobayashi, Y.; Cheong, S. H.; Karube, I. *Chem. Lett.* **1997**, 1297−1298.

(33) Brunauer, S.; Emmett, P. H.; Teller, E. *J. Am. Chem. Soc.* **1938**, *60*, 309−319.

(34) Barret, E. P.; Joyner, L. G.; Halenda, P. P. *J. Am. Chem. Soc.* **1951**, *73*, 373−380.

(35) Kinetic studies performed in solution with non-vinyl analogues of **1** have shown that ligand-exchange reactions proceed faster when water is present (manuscript in progress). A large excess of H_2O was added to all MIP ligand-exchange reactions to ensure that they were performed under identical, water-saturated conditions.

(36) This polymer was dried at 150 °C to remove all traces of PhCl before elemental analysis. All other polymers used in rebinding experiments were dried at room temperature.

hexanes) of the final Soxhlet extract showed that 13.2 μmol of BINOL (56.1% of the total Pt sites in **P4**-rebound; 66.6% ee) and an additional 3.56 μmol of (*R*)-Bu_2BINOL [15.2% of the total Pt sites in **P4**-rebound; total, (*R*)-Bu_2BINOL was removed from 84.3% of the Pt sites of the original **P1**] were recovered from the polymer.

Rebinding Time or Temperature Experiments (Figures 1 and 2). A single batch of **P3** was divided into six parts, each of which was subjected to the *rac*-BINOL rebinding reaction under identical conditions except for rebinding time or temperature.

Typical Sequential Rebinding Experiment (Table 1). PhCl (2 mL) and water (0.5 mL) were added to a flask equipped with a reflux condenser and charged with **P3** [0.40 g, 52.0 μmol of total Pt, 34.8 μmol of $Pt(OAr)_2$] and *rac*-BINOL (129 mg, 451 μmol). The reaction mixture was stirred for 4 h at 60 °C under Ar. The polymer was then filtered from hot solution, transferred to a glass Soxhlet thimble, and extracted with CH_2Cl_2 for 10 h. After drying in vacuo for 2 h at 50 °C, 0.40 g of yellow **P4**-rebound was obtained. To a flask containing this polymer and 201 mg of *rac*-Br_2BINOL (452 μmol) were added 2 mL of PhCl and 0.5 mL of H_2O, and the mixture was stirred for 4 h at 60 °C under Ar. The polymer was again filtered from hot solution, transferred to a glass Soxhlet thimble, and extracted with CH_2Cl_2 for 18 h. After drying in vacuo for 4 h, 0.39 g of yellow **P4/5**-rebound was obtained. Finally, this polymer was cleaved with HCl to give **P2**. Quantitative chiral HPLC analysis (OD-H column, 5% EtOH/hexanes) of the final Soxhlet extract showed that 10.1 μmol of BINOL (20.0% of the total Pt sites in **P4/5**-rebound; 88.8% ee), 20.7 μmol of Br_2BINOL (40.9% of the total Pt sites in **P4/5**-rebound; 46.4% ee), and an additional 8.2 μmol of (*R*)-Bu_2BINOL [16.1% of the total Pt sites in **P4/5**-rebound; total, (*R*)-Bu_2BINOL was removed from 82.9% of the Pt sites of original **P1**] were recovered from the polymer.

Acknowledgment. N.M.B. thanks the UNC Board of Governors and the ACS Division of Organic Chemistry (sponsored by the Rohm & Haas Co.) for Graduate Fellowships. This work was partially supported by the NSF (CAREER, CHE-9624852); the Petroleum Research Fund, administered by the ACS; the DuPont Co., through a Grant in Aid; the 3M Corp., through an Untenured Faculty Research Award; and the UNC University Research Council. We also gratefully acknowledge Prof. R. G. Bergman for helpful discussions while on sabbatical at UNC.

Supporting Information Available: Complete experimental procedures and characterization data for **1** and precursors (PDF). This material is available free of charge via the Internet at *http://pubs.acs.org*. See any current masthead page for ordering information and Web access instructions.

JA000462C